# The Influence of Initial Target Surface State and Irradiation Parameters on the Micro-Craters Formation

A.Y. Leyvi, A.E. Mayer*, V.A. Shulov**, and A.P. Yalovets*

*Institute of Electrophysics RAS, Ural Branch, 106, Amundsen str., Ekaterinburg, 620016, Russia*
*Phone, Fax: +8(315) 267-91-40*
**South-Ural State University, 76, Lenina ave., Chelyabinsk, 454080, Russia*
***Moscow Aviation Institute, 4, Volokolamskoye shosse, Moscow, 125871, Russia*

**Abstract – The numerical investigation of the statistical regularities of micro-craters formation on irradiated target surface has been carried out in comparison with experimental results. The mathematical model of craters formation bases on Taylor instability of the irradiated surface is presented. It has been shown that the separate crater size and form depend on the irradiation regime and on the target material mainly, while the craters distribution density depends on the initial target surface relief. It has been shown that the foreign inclusions (phase insertions) with the mass density different from the basic target material are able to initiate cratering as well as the geometrical perturbations of the irradiated surface relief. The craters induced by foreign inclusions are indistinguishable in form and size from the induced by surface perturbations craters.**

## 1. Introduction

The solid targets processing by the powerful charged particle beams with power density $\geq 10^6$ is widely used for the properties modification of the broad nomenclature of details. Radiation processing is used often as the tool for smoothing of details and targets [1, 2]. But the radiation processing can also lead to the negative results such as the micro-crater formation on the target surface [3–5]. It is well known that the irradiation regime and the initial physical-chemical state of target surface play an important role in the crater formation.

The influence of radiation regime on the distribution density $n_C$ and average size of craters was experimentally investigated in [3] in detail. The surface of titanium alloy BT9 has been irradiated in "TEMP" facility [6] by the powerful ion beam (PIB) with particle energy $U_b = 300$ keV, pulse duration $\tau_b = 50$ ns, and current density $j_b = 60 \div 180$ A/cm$^2$ (70% – carbon ions, 30% – protons) in this work. The next conclusions are followed from [3]: 1) there is a current density threshold for cratering, this threshold depends on the number of pulses $N_p$ and slightly decreases with the grow of $N_p$; 2) craters distribution density $n_C$ depends on the current density $j_b$ and on the number of pulses $N_p$ not monotonically; 3) craters depth reaches $1 \div 2$ μm, while they diameter varies from ~ 1 μm up to ~ 100 μm; 4) the previous mechanical processing (it means the initial relief of target) effects substantially on the craters distribution density.

The existence of energy density threshold for cratering and the substantial influence of initial relief have been confirmed by the results of [4, 5] as well, there the targets made from steel and titanium alloy BT8 has been irradiated by the high-current electron beam (HCEB) with electrons energy $U_b = 115 \div 120$ keV, pulse duration $\tau = 25 \div 50$ μs and energy density $W = 15 \div 50$ J/cm$^2$.

The cratering at irradiation is the result of Taylor instability development on irradiated surface, as it has been shown in [7, 8]. The previous theoretical publications [7, 8] have been directed on the single crater dynamic investigation. The dependence of distribution density and crater sizes on the irradiation regimes and initial target surface state (statistical regularities of cratering) has been numerically investigated in present report. Furthermore, analysis of the foreign inclusions (phase insertions) influence on the cratering has been carried out.

## 2. Physical and mathematical model

There are two regimes of irradiation differing qualitatively in the target substance response: subcritical and supercritical, as it have been noted in [8]. Supercritical regime is characterized by the formation and intensive expansion of plasma layer with velocities up to $100 \div 1000$ m/s at target surface, which leads to the Taylor instability development on the irradiated surface. Subcritical regime precedes supercritical one, it is characterized by relatively slow thermal expansion of solid or liquid (but not plasma) surface layer of target with velocities $1 \div 10$ m/s and leads to the surface relief smoothing [9]. The transition from subcritical regime to supercritical one has the threshold character on energy density.

There was not accounting of surface tension and viscosity in [7, 8]. The more precise mathematical model was offered in [9], this model improves the mentioned limitations. But the work [9] itself was dedicated to investigation of the surface smoothing (in subcritical regimes of irradiation). We use here the mathematical model from [9] generalized for the foreign inclusions accounting.

The target at irradiation consists of the plasma layer, the deeper liquid melt and the main solid part of the target in general case. The rapid plasma layer expansion causes the Taylor instability development, its substance removes from the target afterwards. The plasma-liquid interface forms the final target relief after the melt crystallization. Let us factor the plasma and liquid region into the $L$ layers and suppose the flow in every one of them to be potential and incompressible [9]. Then we can write the Lagrange equations with generalized coordinates $a_i$ is the perturbation amplitudes of interfaces between the layers. The Lagrange function takes into account inertia forces and surface tension, while the dissipative function takes into account viscosity.

Foreign inclusions in surface layer can provoke the target relief deformation even in case of initially flat surface and absolutely uniform irradiation. This deformation is connected with non-homogeneity of inertia forces in the target bulk. Inclusions are trapped in the target substance by friction (viscosity).

Therefore, we neglect their relative movement and consider them as a unified substance with non-homogeneous density. Let us consider the harmonic perturbation $\rho^{(1)}(z,t)\cos(kx)$ superimposed on the uniform along $x$ ("unperturbed") distribution $\rho^{(0)}(z,t)$. Then we obtain the next equations system:

$$\begin{aligned}&\beta_{i-1/2}\ddot{a}_{i-1}+\beta_i\ddot{a}_i+\beta_{i+1/2}\ddot{a}_{i+1}=\alpha_{i-1/2}a_{i-1}+\\&+(\alpha_i-k^2\sigma_i)a_i+\alpha_{i+1/2}a_{i+1}-\\&-(\gamma_{i-1/2}+\dot{\beta}_{i-1/2})\dot{a}_{i-1}-(\gamma_i+\dot{\beta}_i)\dot{a}_i\\&-(\gamma_{i+1/2}+\dot{\beta}_{i+1/2})\dot{a}_{i+1}-\varphi_i,\quad i=0,L-1,\end{aligned}\tag{1}$$

here points denote the time derivatives. The next notations are used in (1) also:

$$\alpha_i=g_i\left(\rho_{i+1/2}-\rho_{i-1/2}\right);\ \beta_{i+1/2}=-\frac{1}{k}\rho_{i+1/2}\frac{1}{\mathrm{sh}(kh_{i+1/2})};$$

$$\beta_i=\frac{1}{k}\left[\rho_{i-1/2}\,\mathrm{cth}(kh_{i-1/2})+\rho_{i+1/2}\,\mathrm{cth}(kh_{i+1/2})\right];$$

$$\gamma_i=4k\left[\eta_{i-1/2}\,\mathrm{cth}(kh_{i-1/2})+\eta_{i+1/2}\,\mathrm{cth}(kh_{i+1/2})\right];$$

$$\gamma_{i+1/2}=4k\left[-\frac{\eta_{i+1/2}}{\mathrm{sh}(kh_{i+1/2})}\right];\ \varphi_i=\varphi_{i+1/2}+\varphi_{i-1/2};$$

$$\varphi_{i+1/2}=\frac{g_{i+1/2}\rho^{(1)}_{i+1/2}}{k}\frac{\mathrm{ch}(k\cdot h_{i+1/2})-1}{\mathrm{sh}(k\cdot h_{i+1/2})}.$$

Here $\rho_{i+1/2}$ and $\eta_{i+1/2}$ are the mass density and the dynamic viscosity coefficient of the layer with number $i+1/2$; $\sigma_i$ is the surface tension coefficient of the $i$th interface between layers; $h_{i+1/2}=z_{i+1}-z_i$ is the layer thickness; $g_i$ is the local acceleration of target substance (its direction is opposite to the inertia forces); $k=2\pi/\lambda$ is wavenumber of perturbation. Boundary conditions: $a_{-1}=0$ is the vacuum over the target and $a_L=0$ is the fixed bottom of the melt. Equation system (1) is valid only in frames of linear approximation $a_ik\ll 1$ and $(a_i\rho)(\partial\rho/\partial z)\ll 1$.

We use the 1D simulations of the target irradiation by BETAIN1 numerical code [10] for the obtaining of mass density and acceleration depth distributions, as it was done in [9]. This code solves jointly the kinetic equation for the fast particles of the beam, the 1D mechanics of continua equations (in the frames of the elastic-plastic model), equations for heat conductivity, melting and crystallization, and the wide-range equation of state.

### 3. Statistical regularities of cratering

Nonlinear effects determine the depth and interaction (junction and fragmentation) of craters only [8]. Therefore, linear approximation was used for the investigation of statistical regularities of cratering. The target surface relief was expanded in a Fourier series, and every Fourier component evolves according with equations (1). The surface final state is obtained as a superposition of all Fourier components with amplitudes corresponding to the moment of crystallization.

The perturbation spectrum normalized on the initial perturbation amplitude ("grow function") is shown in Fig. 1 at the moment of crystallization (titanium target, PIB with parameters corresponding to "TEMP" facility, $N_p=1$).

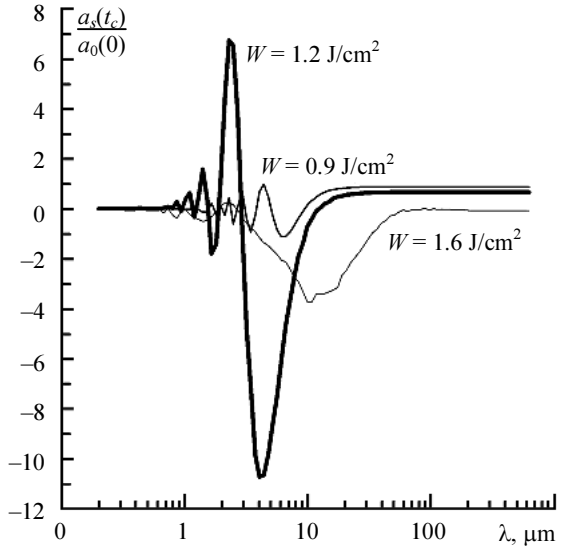


Fig. 1. The calculated grow functions for different energy densities, irradiation by PIB ("TEMP")

Oscillation period is more than crystallization time for the long-wavelength components ($\lambda\geq 20\div 30$ μm), and their amplitudes change weakly over a pulse. An intensive viscose damping takes place for $\lambda\leq 1\div 3$ μm providing the smoothing of such short-wavelength components.

The most essential is the middle wavelengths interval ($\lambda\approx 2\div 30$ μm), the amplitude of such components does not exceed initial value in subcritical

regime ($w$ = 0.9 J/cm$^2$), while in supercritical regime this amplitude can exceed initial value in several times.

There are no craters after one pulse of irradiation ($N_p$ = 1) with energy density $W$ = 0.9 J/cm$^2$ (the subcritical irradiation regime) in experiments [3]. But there is a cratering after three pulses ($N_p$ = 3) with the same energy density. A possible cause cans consist in fluctuations of the beam current and voltage, which lead to transition in supercritical regime during a one pulse of irradiation at least.

Let's consider a quadrate target surface area 1mm×1mm for the integral cratering picture analysis. Its initial relief has been set stochastically: initial amplitudes of the Fourier components have been selected from the interval ($–A_0/N$, $A_0/N$) with the uniform probability, here $A_0$ = 1 μm is the initial target roughness, $N$ is the number of Fourier components.

An integral picture of surface modification is shown in Fig. 2. It corresponds to the iron target irradiation by HCEB. The spectrum modification and the substantial growth of roughness (from 1 to 20 μm) are clearly visible.

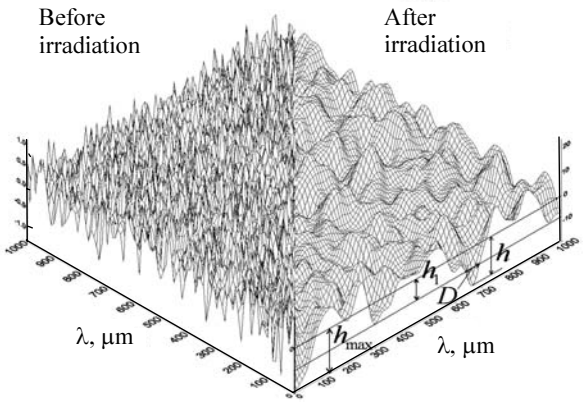


Fig. 2. Initial target surface (Fe) and surface after the processing by HCEB with parameters τ = 2 μs, $U_b$ = 40 keV, $j_b$ = 35 A/cm$^2$ (numerical simulation)

We estimate the number and sizes of craters. Cavities with the depth higher than $h_1$ have been identified as craters (Fig. 2), here $h_1 = ch_{max}$, $h_{max}$ is the maximal depth of cavities and $c$ = 0.85 is the empirical constant matched to experimental data [3]. We use the sample containing 100 different random initial surfaces (similar to Fig. 3) to determine average values and deviations of the crater distribution density $n_C$, diameter $D$, and depth $h$.

The numerical simulations show that the crater distribution density weakly depends on the beam energy density (Figs. 3, *a* and *b*), that is matched to experimental data.

There are the crater average diameter $D$ dependencies on the PIB energy density for the different number of pulses on Figs. 3, *c* and *d*. There is the maximum of average diameter at $W$ = 1.3 J/cm$^2$. This maximum is explained by the increase of plasma layer expansion at the energy density increase. It causes the large

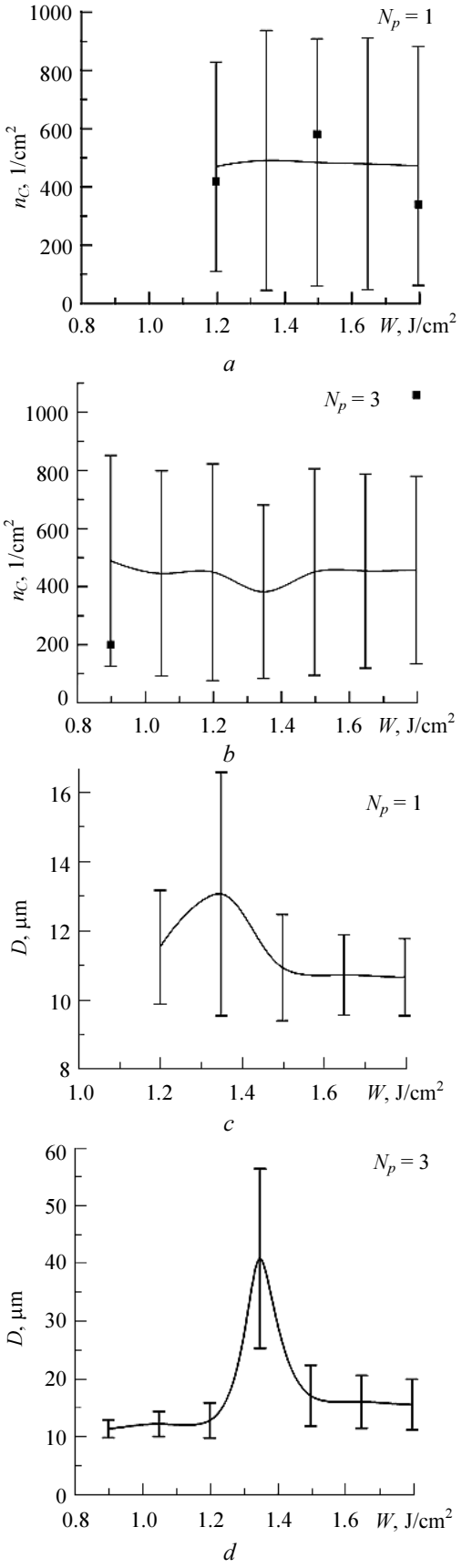


Fig. 3. Craters distribution density (*a* and *b*), and diameters (*c* and *d*) versus the energy density (Fe target, PIB – "TEMP"); markers – experimental points [3]

values of acceleration on the one hand, and the weakening of free surface influence on the deeper layers of target on the other hand. Balance between these two tendencies leads to the maximum.

There are calculation results for the HCEB irradiation with parameters corresponding to facility [1, 2] in Fig. 4.

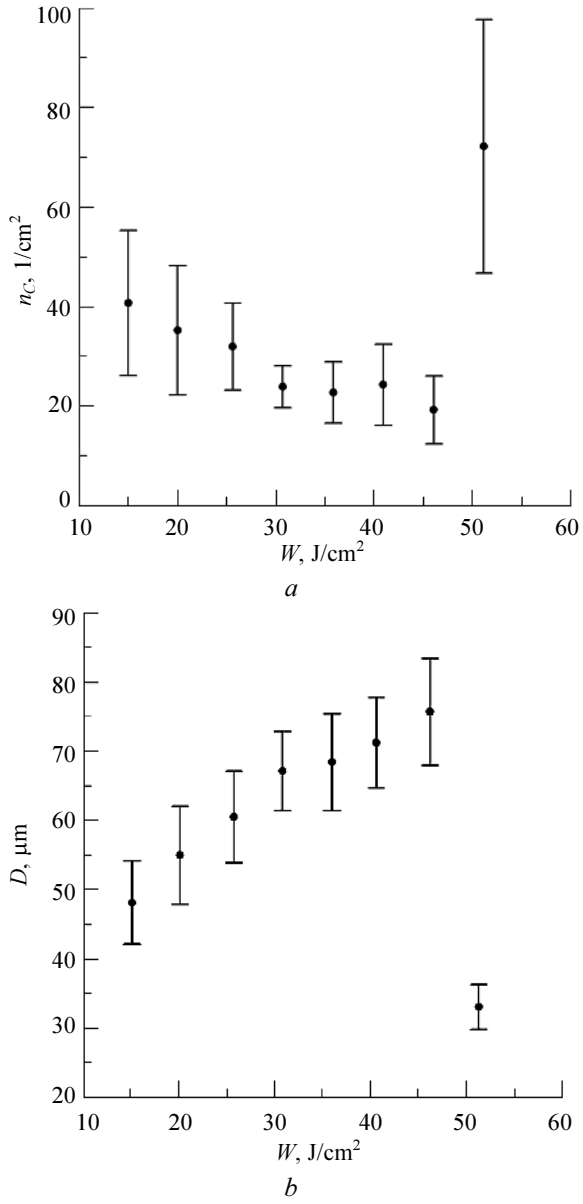


Fig. 4. Craters distribution density (*a*) and diameter (*b*) versus the energy density (Fe target, HCEB: $\tau = 2$ μs, $U_b = 40$ keV, $W = 15 \div 50$ J/cm$^2$)

The energy density increase elongates the melt stage and makes the molten layer deeper on the one hand. Therefore, the crater diameter increase till the $W = 46$ J/cm$^2$. But the mass removed from target in plasma torch increases as well on the other hand. Therefore, the further increase of energy density leads to the growth of craters distribution density and to the reduction of their diameters. The calculation results are in agreement with the common experimental regularities [1, 3, 5] concerning the target surface modification under the HCEB irradiation.

## 4. Foreign inclusions and cratering

The induced by foreign inclusions instability have been simulated with use of linear theory (1) during the irradiation. The crater development after the irradiation has been simulated by the local mapping method [11], which allows for nonlinear effects.

An analysis shows that the inclusions of different density are able to provoke the cratering through the Taylor instability development. Inclusion must be localized in the ablating by irradiation surface layer to provoke the crater. The cratering regularities in this case are similar to such regularities in case of the surface relief perturbations.

The craters induced by foreign inclusions are similar in form and size with the craters induced by surface perturbations. It is obvious from Fig. 5, there the resulting crater profiles are presented.

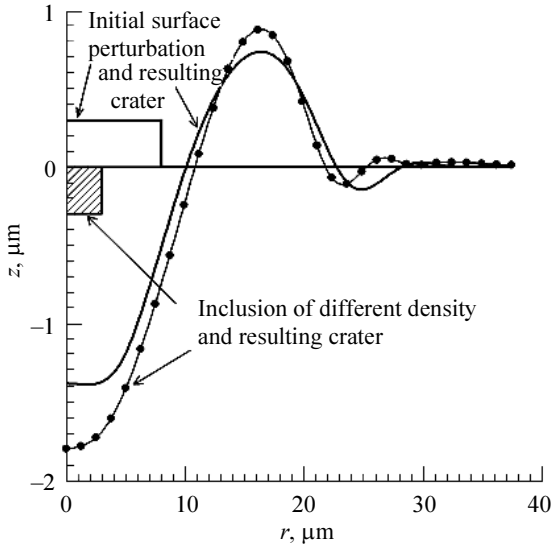


Fig. 5. Profiles of craters initiated by surface relief perturbation and by foreign inclusion. Titanium target; PIB ("TEMP"): $\tau = 50$ ns, $T_b = 250$ KeV, $j_b = 200$ A/cm$^2$

One of them is initiated by the cylindrical microprojection with the height 0.3 μm and radius 8 μm. Another one is provoked by the cylindrical inclusion with radius 3 μm and depth 0.3 μm and with the normalized difference of density $\xi = (\rho_0 - \rho_k)/\rho_0 = 0.4$ located under the flat target surface (here $\rho_k$ is the density of inclusion, $\rho_0$ is the density of target substance).

## 5. Conclusions

The dominant role of Taylor instability in cratering at electron and ion irradiation has been confirmed. The numerically obtained threshold in energy density between subcritical and supercritical regimes of irra-

diation corresponds with the experimentally revealed threshold of cratering.

The separate crater size and form are determined by the irradiation regime and by the target material mainly, while the craters distribution density (in supercritical regime) is determined by the initial target surface relief for the most part.

Foreign inclusions with the mass density different from the basic target material are able to initiate cratering. Inclusion must be localized in the ablating by irradiation surface layer. The craters induced by foreign inclusions are indistinguishable in form and size from the craters induced by surface perturbations.

It is necessary to process targets in subcritical regime of irradiation ore to complete the multi-stage processing by the final cycles in subcritical regime to eliminate cratering.

**References**

[1] P. Raharjo, K. Uemura, A. Okada, and Y. Uno, *in Proc. 7th Int. Conf. on Modification of Materials with Particle Beams and Plasma Flows*, 2004, pp. 263–266.

[2] P. Raharjo, K. Uemura, A. Okada, and Y. Uno, *in Proc. 7th Int. Conf. on Modification of Materials with Particle Beams and Plasma Flows*, 2004, pp. 267–270.

[3] V.A. Shulov, *Modification of the heat-resistant alloy's properties by the contin. and pulsing ion beams, Thesis for a Doctor's degree*, Minsk, 1995.

[4] A.G. Paikin, V.A. Shulov, V.I. Engelko et al., Rus. Uprochn. Technol. Pokrytiya **10**/22, 9 (2006).

[5] A.G. Paikin, V.A. Shulov, V.I. Engelko et al., Rus. Uprochn. Technol. Pokrytiya **1**/25, 3 (2007).

[6] D.R. Akerman, N.F Isakov, and G.E. Remnev, *in Proc. 1th Conf. on Modification of the Properties of Constructional Materials by Charged-Particle Beams, Part 1*, 1988, p. 3.

[7] N.B. Volkov, A.E. Mayer, and A.P. Yalovets, Zh. Tekh. Fiz. **47**, 968 (2002).

[8] N.B. Volkov, A.E. Mayer, K.A. Talala, and A.P. Yalovets, Pis'ma Zh. Tekh. Fiz. **32**, 424 (2006).

[9] V.S. Krasnikov, A.Y. Leivy, A.E. Mayer, and A.P. Yalovets, Rus. Zh. Tekh. Fiz. **52**, 431 (2007).

[10] A.P. Yalovets and A.E. Mayer, *in Proc. 6th Int. Conf. on Modification of Materials with Particle Beams and Plasma Flows*, 2002, pp. 297–299.

[11] N.B. Volkov, A.E. Mayer, and A.P. Yalovets, Zh. Tekh. Fiz. **48**, 275 (2003).